CHEMIJA. 2016. Vol. 27. No. 1. P. 31–36

Pt-CeO_2/C and Pt-Nb_2O_5/C as electrocatalysts for ethanol electro-oxidation

Virginija Kepenienė*,

Loreta Tamašauskaitė-Tamašiūnaitė,

Jūratė Vaičiūnienė,

Vidas Pakštas,

Eugenijus Norkus

Department of Catalysis,
Center for Physical Sciences and Technology,
A. Goštauto St. 9,
LT-01108 Vilnius, Lithuania

The aim of this study was to investigate the activity of CeO_2/C and Nb_2O_5/C supported platinum nanoparticles composites, prepared by the rapid microwave synthesis method, towards the oxidation of ethanol in an alkaline medium. The electrocatalytic activity of the Pt-CeO_2/C and Pt-Nb_2O_5/C catalysts with respect to the electro-oxidation of ethanol was investigated by means of cyclic voltammetry. The electrochemical behaviour of the synthesized catalysts towards the oxidation of ethanol was compared with that of a carbon supported bare Pt catalyst. X-ray Diffraction and Transmission Electron Microscopy were used to determine the structure, shape and the size of catalysts particles. Inductively Coupled Plasma Optical Emission Spectroscopy (ICP-OES) was employed to determine the composition of the synthesized catalysts.

It has been found that the both investigated Pt-CeO_2/C and Pt-Nb_2O_5/C catalysts show a higher activity towards the electro-oxidation of ethanol when compared with that of the Pt/C catalyst, the Pt- Nb_2O_5/C catalyst being most active.

Keywords: platinum, cerium(IV) oxide, niobium(V) oxide, electrocatalysts, ethanol electro-oxidation

INTRODUCTION

Proton exchange membrane fuel cells (PEMFCs) have been widely investigated over several decades as one of the most promising alternative power sources [1–4]. Recently, much interest has been attracted to the use of alcohols in fuel cells. The authors predominantely studied direct methanol fuel cells (DMEFCs) [5–7], however, there is evidence that methanol may be replaced by environment-friendly ethanol and may be successfully used in direct ethanol fuel cells (DEFCs) [8–11]. The low toxicity, light enough availability (from biomass products) and transportation makes ethanol a promising alternative fuel [12–15].

Since the start of the fuel cell trials, platinum-supported materials were among the most commonly used ones. However, researchers have been looking for ways to reduce the amount of platinum in the catalysts because of its high cost and possible poisoning of the electrode surface. Therefore, recently research has been focused on a new generation of catalysts, where part of platinum is modified by addition of other metals (Au, Co, Ni, Ru, Pd etc.) [16–20] or rare earth and transition metal oxides (Al_2O_3, CeO_2, TiO_2 etc.) [21–28]. It was reported that directly added metal oxides such as Al_2O_3 [21, 22], CeO_2 [23–26], TiO_2 [27–29] promote electrocatalytic properties of catalysts towards the oxidation of ethanol and methanol as compared to those of bare Pt catalysts and allow reducing the Pt amount in the catalysts. Rare earth metal oxide, such as CeO_2, is widely used as an additive in preparation of fuel cell catalysts due to its synergetic electronic effect, tolerance to CO poisoning, low price and many other characteristics [30–32]. To our knowledge, a very few works describe the use of Nb_2O_5 oxide as a support for deposition of well-dispersed Pt nanoparticles for ethanol electro-oxidation, although it has excellent properties such as chemical stability and corrosion resistance. Justin et al. and Chun et al. [33, 34] have investigated the electrochemical oxidation of methanol on Pt-Nb_2O_5/C in acidic media and described the enhanced electrocatalytical properties of the latter catalyst as compared to those of the Pt/C catalyst.

In this study the Pt supported CeO_2/carbon and Nb_2O_5/carbon catalysts (denoted as Pt-CeO_2/C and Pt-Nb_2O_5/C) were prepared by means of microwave synthesis [35, 36]. The prepared catalysts were characterized by means of X-ray Diffraction (XRD), Transmission Electron Microscopy

* Corresponding author. E-mail: virginalisk@gmail.com

(TEM) and Inductively Coupled Plasma Optical Emission Spectroscopy (ICP-OES). The electrocatalytic activity of the synthesized catalysts towards the ethanol oxidation reaction was investigated by cyclic voltammetry.

EXPERIMENTAL

Chemicals

H_2PtCl_6 (37.5%), Nb_2O_5 powder (purity 99.9%), CeO_2 powder (purity 99.95%) and graphite powder (99.9995%) were purchased from Alfa-Aesar and Aldrich suppliers. Nafion (5 wt.%, D521, 1100 EW) was purchased from Ion Power Inc. Supply. H_2SO_4 (96%), NaOH (98.8%), ethanol (96%), glycerol (99.5%) and acetone (99.5%) were purchased from Chempur Company. All chemicals were of analytical grade. Ultra-pure water with the resistivity of 18.2 MΩ cm^{-1} was used to prepare all the solutions.

Preparation of catalysts

The primary CeO_2/C and Nb_2O_5/C composites were prepared according to the following procedures: at first, dry powders of CeO_2 or Nb_2O_5 were mixed with carbon (mass ratio being 1:1) in a 2-propanol solution by ultrasonication for 30 min with further desiccation of the mixture. Further, CeO_2/C and Nb_2O_5/C composites were heated at 500 °C for 2 h. Later, Pt nanoparticles were dispersed over CeO_2/C and Nb_2O_5/C composites by the rapid microwave heating method. The typical preparation consists of the following steps: at first, a solution containing 1.9 mM of H_2PtCl_6 and 1 M of glycerol was prepared. pH of the solution was adjusted to 11.65 by adding dropwise a 0.4 M NaOH solution. Then, 100 mg of CeO_2/C or Nb_2O_5/C was added to the solution mentioned above and it was sonicated for 20 min. Then the prepared reaction mixture was put into a microwave reactor Monowave 300 (Anton Paar). Synthesis was carried out at a temperature of 170 °C for 30 s. For comparison purposes, the carbon supported Pt catalyst was also prepared under the same conditions. After preparation, the synthesized catalysts were washed with acetone, ultrapure water with the resistivity of 18.2 MΩ cm^{-1}, then filtered and dried in a vacuum oven at 80 °C for 2 h.

Characterization of catalysts

The shape and size of catalyst particles were examined using a transmission electron microscope Tecnai G2 F20 X-TWIN equipped with an EDAX spectrometer with an r-TEM detector. For microscopic examinations, 10 mg of sample was first sonicated in 1 ml of ethanol for 1 h and then deposited on a Cu grid covered with a continuous carbon film.

X-ray diffraction patterns were recorded using a D8 diffractometer (Bruker AXS, Germany) with Cu Kα radiation using a Ni/graphite monochromator. A step-scan mode was used in the 2-theta range from 20 to 90° with a step length of 0.02° and a counting time of 5 s per step.

The Pt metal loadings were estimated from ICP-OES measurements. The ICP optical emission spectra were recorded using an ICP optical emission spectrometer Optima 7000DV (Perkin Elmer).

Electrochemical measurements

Ethanol electro-oxidation measurements were performed with a Zennium electrochemical workstation (ZAHNER-Elektrik GmbH & Co. KG) using a three-electrode cell. A thin layer of the prepared Pt-CeO_2/C, Pt-Nb_2O_5/C and Pt/C catalysts deposited on a glassy carbon electrode with a geometric area of 0.07 cm^2 was used as a working electrode, a Pt wire was used as a counter electrode and an Ag/AgCl/KCl (3 M KCl) electrode was used as a reference. Steady state linear sweep voltammograms were recorded in a 1 M C_2H_5OH + 0.5 M NaOH solution at a linear potential sweep rate of 50 mV s^{-1} from –0.5 to 0.5 V at a temperature of 25 °C. The electrode potential is quoted versus the standard hydrogen electrode (SHE). The presented current densities are normalized with respect to the geometric area of catalysts. All solutions were deaerated by argon for 15 min prior to measurements.

The working electrode was prepared according to the following steps: at first, 10 mg of the Pt-CeO_2/C, Pt-Nb_2O_5/C or Pt/C catalysts was dispersed ultrasonically for 1 h in a solution containing 0.25 µl of 5 wt.% Nafion and 0.75 µl deionized H_2O to produce a homogeneous slurry. Then, 5 µl of the prepared suspension mixture was pipetted onto the polished surface of a glassy carbon electrode and dried in air for 12 h.

RESULTS AND DISCUSSION

One of the reactions taking place in DEFC is ethanol oxidation, so it is very important to develop an effective and selective catalyst for this reaction. It is known that the rare earth metal oxides enhance electrocatalytic activity of catalysts towards the oxidation of ethanol. The powders of CeO_2 and Nb_2O_5 oxides are cheaper than pure Pt precursors, so adding them to the catalyst system allows not only reducing the price of the catalysts due to the reduction of the amount of Pt, but also developing more efficient catalysts for ethanol oxidation. In this study the Pt nanoparticles were deposited on the surfaces of carbon, CeO_2/C and Nb_2O_5/C by means of the simple and rapid microwave heating method. The synthesized Pt-CeO_2/C, Pt-Nb_2O_5/C and Pt/C catalysts were examined as electrocatalysts towards the electro-oxidation of ethanol.

Characterization of catalysts

The particle size and shape of synthesized catalysts were determined by Transmission Electron Microscopy. Figure 1 shows the TEM images of the Pt/C (a), Pt-CeO_2/C (b) and Pt-Nb_2O_5/C (c) catalysts. The Pt nanoparticles of ca. 4–5 and 6–12 nm in size were deposited on the surfaces of carbon supported CeO_2 and Nb_2O_5, respectively (Fig. 1b, c). For comparison, the Pt/C catalyst was synthesized with Pt nanoparticles of ca. 2–3 nm in size as depicted in Fig. 1a. In all cases, the Pt nanoparticles were uniform and adequately dispersed on the surface of carbon.

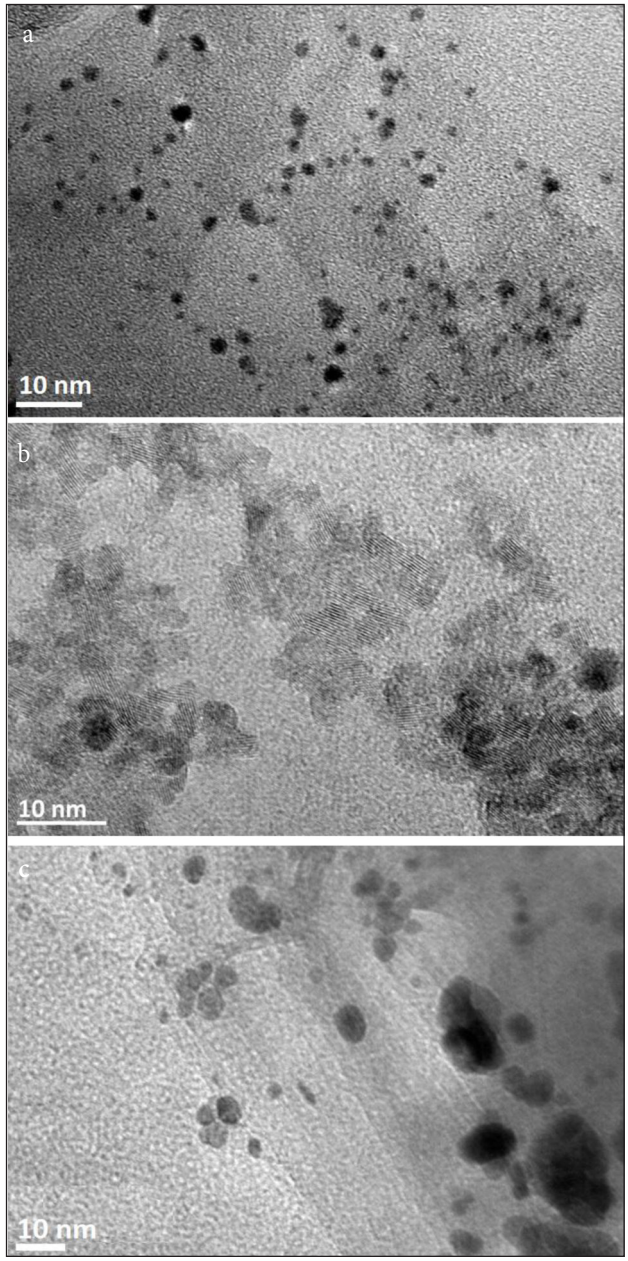

Fig. 1. TEM images of the Pt/C (a), Pt-CeO_2/C (b) and Pt-Nb_2O_5/C (c) catalysts

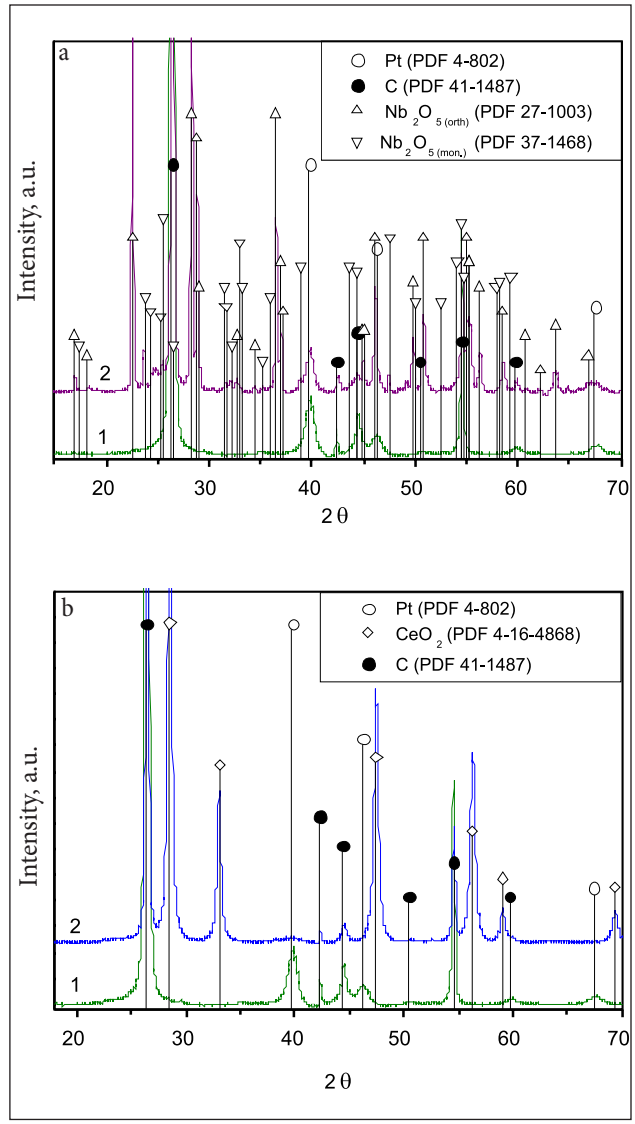

Fig. 2. XRD patterns of the Pt/C (pattern 1, a, b), Pt-Nb_2O_5/C (pattern 2, a) and Pt-CeO_2/C (pattern 2, b) catalysts synthesized by the microwave irradiation method

The crystallographic structures of CeO_2/C and Nb_2O_5/C supported Pt nanoparticles catalysts were estimated by X-ray diffraction measurements. XRD patterns of the synthesized Pt/C, Pt-Nb_2O_5/C and Pt-CeO_2/C are shown in Fig. 2. As seen from the XRD patterns of Pt/C (Fig. 2, pattern 1) and Pt-Nb_2O_5/C (Fig. 2a, pattern 2), the diffraction peaks at the 2θ of 39.76°, 46.24° and 67.45° can be assigned to the characteristic (111), (200) and (220), respectively, crystalline planes of Pt (PDF 4-802). The average size of Pt crystallites in the catalysts was calculated by the Hadler–Wagner method [37]. The average size of Pt nanoparticles deposited on the carbon and Nb_2O_5/C are ca. 4–5 and 12 nm, respectively. It was found that the orthorombic (PDF 27-1003) and monoclinic (PDF 37-1468) Nb_2O_5 particles of ca. 48 and 18 nm in size, respectively, are predominant in the Pt-Nb_2O_5/C catalyst.

Figure 2b shows the XRD patterns of the Pt/C (pattern 1) and Pt-CeO_2/C (pattern 2) catalysts. The Pt (111) diffraction peak at Pt-CeO_2/C is broader than that at Pt/C (Fig. 2, pattern 1) and Pt-Nb_2O_5/C (Fig. 2a, pattern 2), indicating that Pt crystallites are very small (according to TEM), and it is difficult to determine their size correctly. CeO_2 (PDF 4-16-4868) with particles of ca. 16 nm in size was deposited on the surface of carbon.

The Pt loading of the synthesized catalysts was determined by ICP-OES. It has been found that the Pt loadings were 0.128, 0.157 and 0.114 mg Pt cm^{-2} in the Pt/C, Pt-CeO_2/C and Pt-Nb_2O_5/C catalysts, respectively.

Active surface area estimation

The electrochemically active surface areas (ESAs) of Pt in the synthesized catalysts were determined from the cyclic voltammograms of the Pt-CeO_2/C, Pt-Nb_2O_5/C and Pt/C catalysts recorded in a deaerated 0.5 M H_2SO_4 solution at a sweep

rate of 50 mV s^{-1} by calculating the charge associated with hydrogen adsorption (220 μC cm^{-2}) [38] (Fig. 3). It has been determined that the values of ESA are 1.8 cm^2 for Pt/C and 2.7 and 3.5 cm^2 for the Pt-CeO_2/C and Pt-Nb_2O_5/C catalysts, respectively. The specific activity has been determined to be 20 m^2 g^{-1} Pt for Pt/C, 24 m^2 g^{-1} Pt for Pt-CeO_2/C and 44 m^2 g^{-1} Pt for Pt-Nb_2O_5/C.

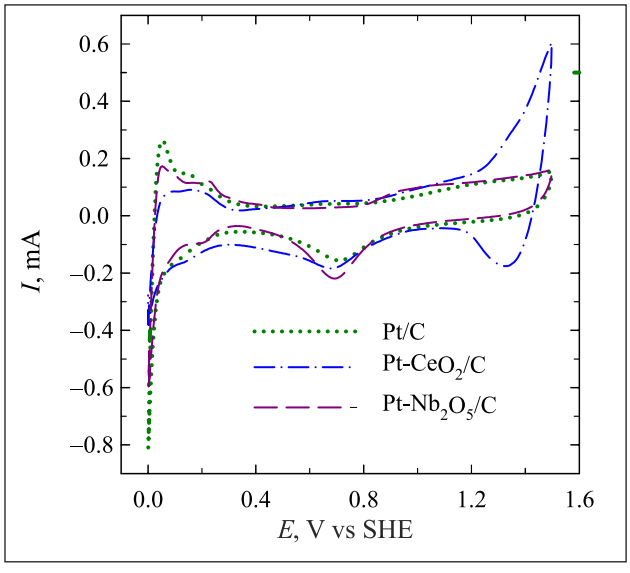

Fig. 3. Cyclic voltammograms of the Pt-CeO_2/C (dash-dotted line), Pt-Nb_2O_5/C (dashed line) and Pt/C (dotted line) catalysts recorded in 0.5 M H_2SO_4 at a sweep rate of 50 mV s^{-1}

Electrocatalytic behaviour of catalysts

The electrocatalytic activity of the Pt-CeO_2/C, Pt-Nb_2O_5/C and Pt/C catalysts with respect to the oxidation of ethanol was investigated by cyclic voltammetry. Figure 4 shows long-term cyclic voltammograms for the Pt-CeO_2/C, Pt-Nb_2O_5/C and Pt/C catalysts recorded in a 1 M C_2H_5OH + 0.5 M NaOH solution at a sweep rate of 50 mV s^{-1}. In the forward sweep, anodic peaks **I** are observed at ca. –0.03 V for the Pt/C and ca. 0 V for the Pt-CeO_2/C and Pt-Nb_2O_5/C catalysts (Fig. 4). Peak **I** is related with the direct oxidation of ethanol in an alkaline medium [36]. In the reverse sweep, anodic peaks **II** were detected at ca. –0.15 V for the Pt/C and ca. –0.10 for the Pt-CeO_2/C and Pt-Nb_2O_5/C catalysts. This peak **II** in the reverse sweep is attributed to the removal of the incompletely oxidized carbonaceous species formed in the forward sweep [39]. During long-term cycling the ethanol electro-oxidation current density values (anodic peak **I**) recorded at the Pt-Nb_2O_5/C catalyst increase in contrast to those at the Pt/C and Pt-CeO_2/C catalysts. However, it should be noted that the obtained first cycle of ethanol oxidation current densities are also greater at the Pt-Nb_2O_5/C catalyst as compared to those at the Pt/C and Pt-CeO_2/C catalysts.

Figure 5 presents stabilized positive potential-going scans (10 cycles) of the investigated catalysts recorded in 1 M C_2H_5OH + 0.5 M NaOH at a sweep rate of 50 mV s^{-1}. As seen

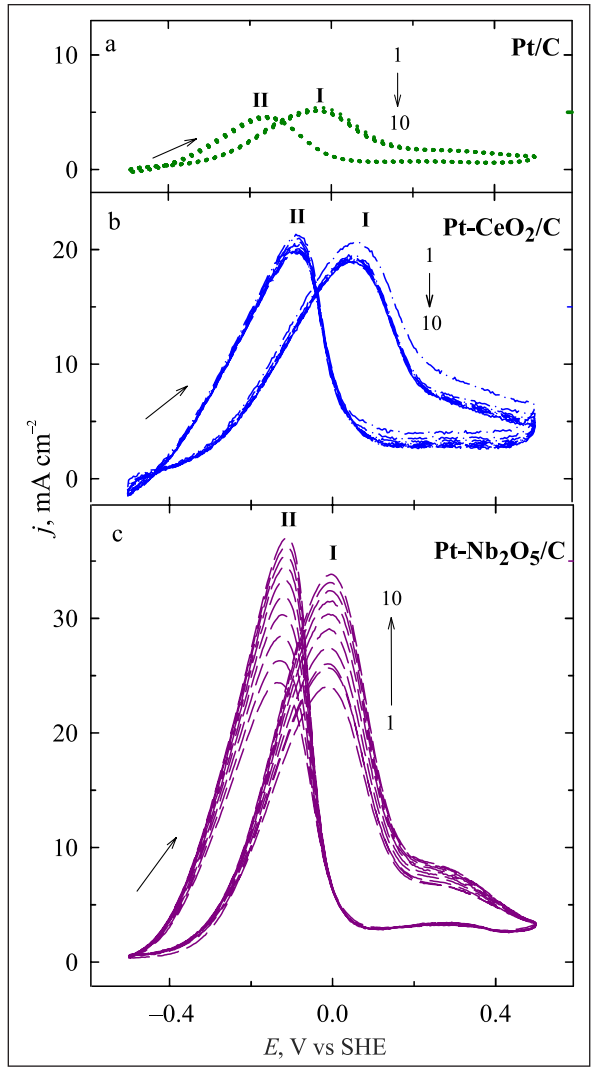

Fig. 4. Cyclic voltammograms of the Pt/C (a), Pt-CeO_2/C (b) and Pt-Nb_2O_5/C (c) catalysts recorded in 1 M C_2H_5OH + 0.5 M NaOH at a sweep rate of 50 mV s^{-1}; at 25 °C

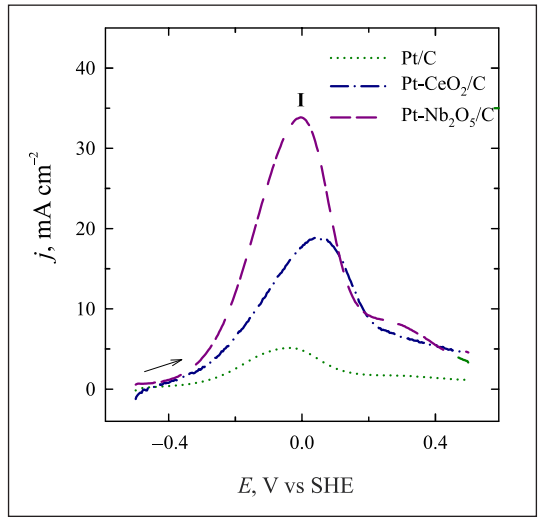

Fig. 5. Stabilized positive-potential going scans (10 cycles) of the Pt-CeO_2/C (dash-dotted line), Pt-Nb_2O_5/C (dashed line) and Pt/C (dotted line) catalysts recorded in 1 M C_2H_5OH + 0.5 M NaOH at a sweep rate of 50 mV s^{-1}

from the data in Fig. 5, the onset potential values on the Pt-CeO_2/C and Pt-Nb_2O_5/C are at ca. 0.1 V more negative as compared to those on the Pt/C catalyst, indicating that CeO_2/C and Nb_2O_5/C promote the oxidation of ethanol on Pt at lower potentials. The obtained ethanol oxidation current densities are also greater at the CeO_2/C and Nb_2O_5/C supported Pt nanoparticles catalysts as compared to those at the bare Pt/C catalyst. Ethanol oxidation current densities are ca. 4 and 6 times higher on the Pt-CeO_2/C (dash-dotted line) and Pt-Nb_2O_5/C (dashed line) catalysts, respectively, as compared to those on the bare Pt/C catalyst (Fig. 5).

To evaluate the electrocatalytic activity of investigated catalysts, ethanol oxidation current densities were normalized by the electrochemically active surface areas and Pt loadings to represent the specific and mass activities of catalysts. Figure 6 shows comparison of current densities (a), specific (b) and mass activities (c) towards the oxidation of ethanol for the prepared catalysts. Assuming ca. 2 times higher ESAs value of the Pt-CeO_2/C and Pt-Nb_2O_5/C catalysts as compared with that of Pt/C, the surface area normalized ethanol oxidation current densities are ca. 2.5 and 3.4 times higher on the Pt-CeO_2/C and Pt-Nb_2O_5/C catalysts, respectively (Fig. 6b).

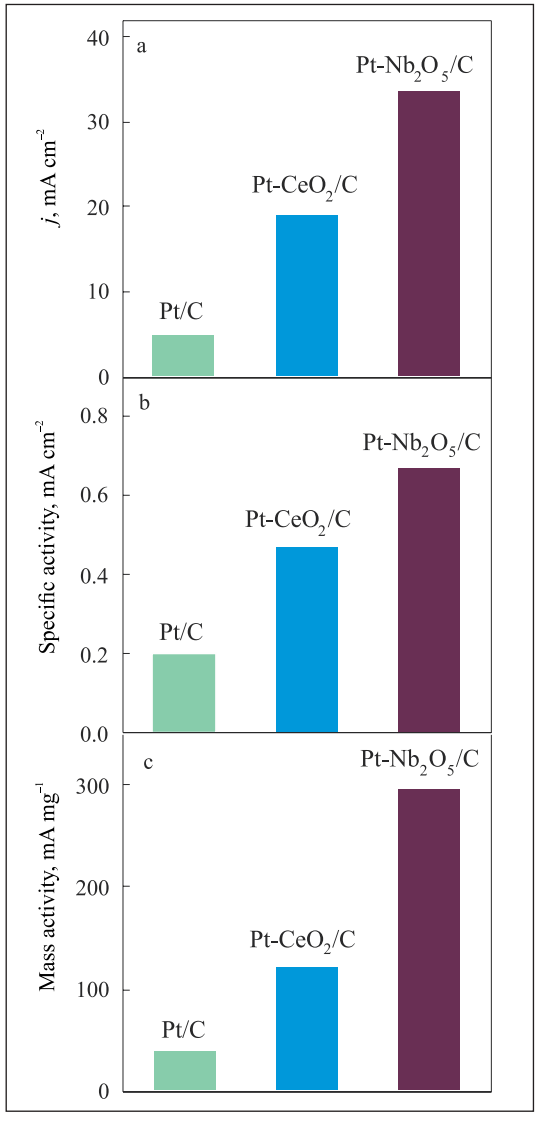

Fig. 6. Comparison of current densities (a), specific (b) and mass activities (c) towards the oxidation of ethanol at 0 V vs SHE for Pt/C, Pt-CeO_2/C and Pt-Nb_2O_5/C recorded in 1 M C_2H_5OH + 0.5 M NaOH at a sweep rate of 50 mV s^{-1}

The mass activities for ethanol oxidation are ca. 3 and 7 times higher at the Pt-CeO_2/C and Pt-Nb_2O_5/C catalysts, respectively, as compared to those at the Pt/C catalyst (Fig. 6c).

It has been found that cerium(IV) oxide/carbon or niobium(V) oxide/carbon supported Pt nanoparticles catalysts show an enhanced electrocatalytic activity towards the electro-oxidation of ethanol in an alkaline medium as compared with that of the carbon supported bare Pt catalyst. A higher activity of Pt-CeO_2/C and Pt-Nb_2O_5/C may be related with the synergistic effect between Pt and CeO_2 or Nb_2O_5 [34, 40–44]. However, the Pt-Nb_2O_5/C catalyst shows the highest catalytic activity among the Pt-CeO_2/C and Pt/C catalysts (Fig. 6). Enhanced activity of Pt-Nb_2O_5/C towards the electro-oxidation of ethanol may be related to the modified electronic structure of Pt by Nb_2O_5 [34]. Furthermore, Nb_2O_5 is well-known for its strong metal–support interaction (SMSI) which shows the pronounced and cooperative effect in metal–metal oxide system [42, 43]. Nb_2O_5 can provide its surface mobile oxygen species to the Pt surface by the spillover effect to facilitate electro-oxidation of adsorbed CO and ethanol [34].

CONCLUSIONS

A rapid microwave heating method was used to prepare the CeO_2/C and Nb_2O_5/C supported Pt nanoparticles catalysts. The Pt nanoparticles of 4–5 and 6–12 nm size were deposited on the CeO_2/C and Nb_2O_5/C supports, respectively.

It has been found that the both investigated Pt-CeO_2/C and Pt-Nb_2O_5/C catalysts show higher activity towards the electro-oxidation of ethanol when compared with that of the Pt/C catalyst. However, the Pt-Nb_2O_5/C catalyst outperforms the Pt-CeO_2/C catalyst towards the electro-oxidation of ethanol and shows the highest electrocatalytic activity in this work.

Received 30 November 2015
Accepted 8 January 2016

References

1. Ch.-Y. Liu, Ch.-Ch. Sung, *J. Power Sources*, **220**, 348 (2012).
2. Z. Wang, H. Tang, H. Zhang, et al., *J. Membr. Sci.*, **421–422**, 201 (2012).
3. S. Song, P. Tsiakaras, *Appl. Catal., B*, **63**, 187 (2006).
4. F. Barbir, T. Gómez, *Int. J. Hydrogen Energy*, **21**, 891 (1996).
5. H. Kunitomo, H. Ishitobi, N. Nakagawa, *J. Power Sources*, **297**, 400 (2015).
6. Ch. Lu, W. Kong, H. Zhang, B. Song, Z. Wang, *J. Power Sources*, **296**, 102 (2015).
7. Z. L. Zhao, L. Y. Zhang, Sh. J. Bao, Ch. M. Li, *Appl. Catal., B*, **174–175**, 361 (2015).

8. C. Lamy, S. Rousseau, E. M. Belgsir, C. Coutanceau, J.-M. Léger, *Electrochim. Acta*, **49**, 3901 (2004).
9. R. Carrera-Cerritos, R. Fuentes-Ramírez, F. M. Cuevas-Muniz, J. Ledesma-García, L. G. Arriaga, *J. Power Sources*, **269**, 370 (2014).
10. M. Morales, F. Espiell, M. Segarra, *J. Power Sources*, **293**, 366 (2015).
11. L. Tsui, C. Zafferoni, A. Lavacchi, M. Innocenti, F. Vizza, G. Zangari, *J. Power Sources*, **293**, 815 (2015).
12. J. Ma, L. Wang, X. Mu, Y. Cao, *J. Colloid Interface Sci.*, **457**, 102 (2015).
13. C. Lamy, A. Lima, V. Le Rhun, F. Delime, C. Coutanceau, J.-M. Léger, *J. Power Sources*, **105**, 283 (2002).
14. E. Peled, T. Duvdevani, A. Aharon, A. Melman, *Electrochem. Solid-State Lett*. **4**, A38 (2001).
15. J. Wang, S. Wasmus, R. F. Savinell, *J. Electrochem. Soc*. **142**, 4218 (1995).
16. V. Kepenienė, L. Tamašauskaitė-Tamašiūnaitė, J. Jablonskienė, et al., *J. Electrochem. Soc.*, **161**, F1354 (2014).
17. L. Tamašauskaitė-Tamašiūnaitė, A. Balčiūnaitė, A. Vaiciukevičienė, A. Selskis, E. Norkus, *J. Power Sources*, **225**, 20 (2013).
18. J.-N. Zheng, L.-L. He, C. Chen, A.-J. Wang, K.-F. Ma, J.-J. Feng, *J. Power Sources*, **268**, 744 (2014).
19. Y. Pan, X. Guo, M. Li, et al., *Electrochim. Acta*, **159**, 40 (2015).
20. H. J. You, F. L. Zhang, Z. Liu, J. X. Fang, *ACS Catal.*, **4**, 2829 (2014).
21. W.-H. Chen, Ch.-T. Shen, B.-J. Lin, Sh.-Ch. Liu, *Energy*, **88**, 399 (2015).
22. J. Zhao, Y. Wang, X. Lou, K. Li, Z. Li, W. Huang, *Inorg. Chim. Acta*, **405**, 395 (2013).
23. M. A. Scibioh, S. K. Kim, E. A. Cho, T. H. Lim, S. A. Hong, H. Y. Ha, *Appl. Catal., B*, **84**, 773 (2008).
24. Y. Zhao, F. Wang, J. Tian, X. Yang, L. Zhan, *Electrochim. Acta*, **55**, 8998 (2010).
25. A. Altamirano-Gutiérrez, A. M. Fernández, F. J. Rodríguez Varela, *Int. J. Hydrogen Energy*, **38**, 12657 (2013).
26. D.-M. Gu, Y.-Y. Chu, Z.-B. Wang, Z.-Z. Jiang, G.-P. Yin, Y. Liu, *Appl. Catal., B*, **102**, 9 (2011).
27. B. Hasa, E. Kalamaras, E. I. Papaioannou, L. Sygellou, A. Katsaounis, *Int. J. Hydrogen Energy*, **38**, 15395 (2013).
28. Y. Zheng, H. Chen, Y. Dai, et al., *Electrochim. Acta*, **178**, 74 (2015).
29. L. Tamašauskaitė-Tamašiūnaitė, A. Balčiūnaitė, A. Vaiciukevičienė, A. Selskis, V. Pakštas, *J. Power Sources*, **208**, 242 (2012).
30. T. Han, Z. Zhang, *Mater. Lett*., **154**, 177 (2015).
31. R. F. B. De Souza, A. E. A. Flausino, D. C. Rascio, et al., *Appl. Catal., B*, **91**, 516 (2009).
32. Y. Wang, A. Tabet-Aoul, M. Gougis, M. Mohamedi, *J. Power Sources*, **273**, 904 (2015).
33. P. Justin, P. Hari Krishna Charan, G. Ranga Rao, *Appl. Catal., B*, **100**, 510 (2010).
34. H.-J. Chun, D. B. Kim, D.-H. Lim, W.-D. Lee, H.-I. Lee, *Int. J. Hydrogen Energy*, **35**, 6399 (2010).
35. S. Liu, L. Wang, J. Tian, et al., *J. Nanopart. Res*., **13**, 4731 (2011).
36. X. Wang, J. Zheng, R. Fu, J. Ma, *Chin. J. Catal*., **32**, 599 (2011).
37. D. Houivet, J. M. Haussonne, in: K. M. Nair et al. (eds.), *Ceramic Materials and Electronic Multilayer Devices*, Vol. 150, The American Ceramic Society, USA (2003).
38. H. Angerstein-Kozlowska, B. E. Conway, W. B. A. Sharp, *J. Electroanal. Chem*., **43**, 9 (1973).
39. R. Manohara, J. B. Goodenough, *J. Mater. Chem*., **2**, 875 (1992).
40. M. C. Orilall, F. Matsumoto, Q. Zhou, et al., *J. Am. Chem. Soc.*, **131**, 9389 (2009).
41. K. Sasaki, L. Zhang, R. R. Adzic, *Phys. Chem. Chem. Phys.*, **10**, 159 (2008).
42. D. A. G. Aranda, M. Schmal, *J. Catal.*, **171**, 398 (1997).
43. P. Marques, N. F. P. Ribeiro, M. Schmal, D. A. G. Aranda, M. M. V. M. Souza, *J. Power Sources*, **158**, 504 (2006).
44. S. Piazza, C. Sunseri, F. D. Quarto, *J. Electroanal. Chem.*, **293**, 69 (1990).

Virginija Kepenienė, Loreta Tamašauskaitė-Tamašiūnaitė, Jūratė Vaičiūnienė, Vidas Pakštas, Eugenijus Norkus

Pt-CeO_2/C IR Pt-Nb_2O_5/C KATALIZATORIAI ETANOLIO ELEKTRO-OKSIDACIJOS REAKCIJAI

S a n t r a u k a

Mikrobangų sintezės metodu buvo suformuoti Pt-CeO_2/C, Pt-Nb_2O_5/C ir Pt/C katalizatoriai, kuriuose nusodintos Pt įkrova atitinkamai lygi 0,157, 0,114 ir 0,128 mg cm^{-2}, o nusodintų Pt nanodalelių dydis minėtuose katalizatoriuose – nuo 2 iki 12 nm.

Darbe tiriamų katalizatorių Pt elektrochemiškai aktyvus paviršiaus plotas buvo nustatomas iš vandenilio monosluoksnio adsorbcijos ant Pt elektrodo krūvio 0,5 M H_2SO_4 tirpale. Nustatyta, kad Pt-CeO_2/C, Pt-Nb_2O_5/C ir Pt/C katalizatoriuose Pt elektrochemiškai aktyvus paviršiaus plotas atitinkamai lygus 2,7, 3,5 ir 1,8 cm^2.

Katalizatorių elektrokatalizinės savybės buvo tiriamos šarminiame etanolio (1 M C_2H_5OH + 0.5 M NaOH) tirpale. Išmatuotos etanolio elektrooksidacijos srovės tankio vertės ant Pt-CeO_2/C ir Pt-Nb_2O_5/C yra 4 ir 6 kartus didesnės nei ant Pt/C katalizatoriaus. Etanolio elektrooksidacijos srovės tankio vertės, normalizuotos pagal nusodintos Pt elektrochemiškai aktyvų plotą ir įkrovą, atitinkamai 3 ir 8 kartus didesnės palyginti su Pt/C katalizatoriumi. Visais tirtais atvejais didžiausiu elektrokataliziniu aktyvumu pasižymėjo Pt-Nb_2O_5/C katalizatorius.